Since January 2020 Elsevier has created a COVID-19 resource centre with free information in English and Mandarin on the novel coronavirus COVID-19. The COVID-19 resource centre is hosted on Elsevier Connect, the company's public news and information website.

Med

CellPress

Clinical and Translational Article

B cell-derived cfDNA after primary BNT162b2 mRNA vaccination anticipates memory B cells and SARS-CoV-2 neutralizing antibodies

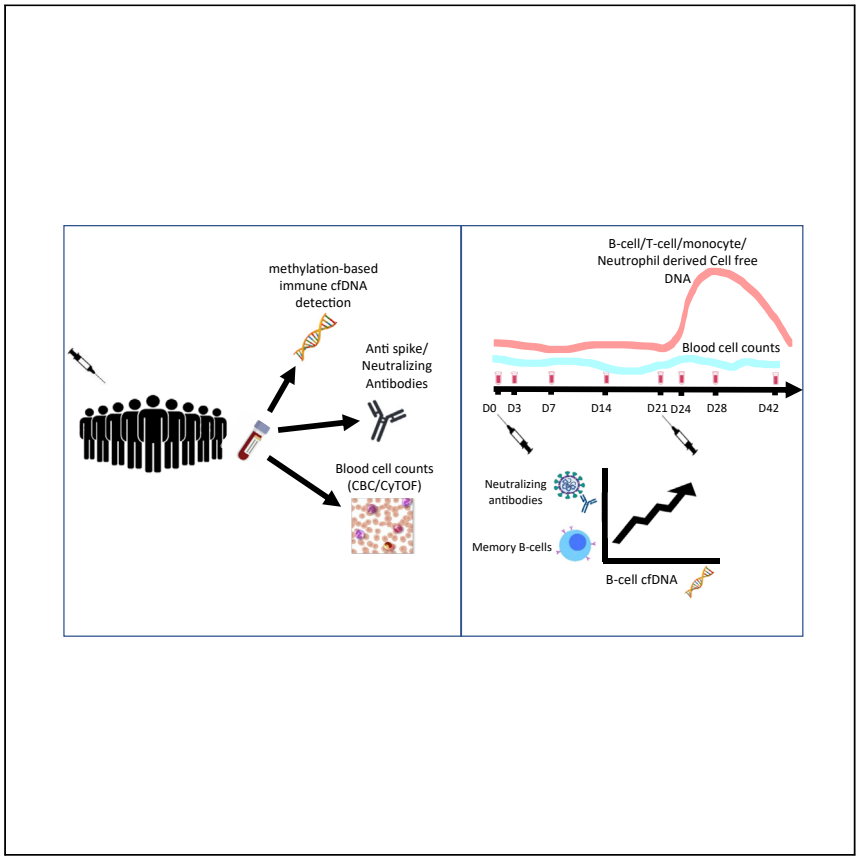

Fox-Fisher and colleagues employed methylation-based cfDNA biomarkers to assess immune cell turnover following SARS-CoV-2 vaccination. The primary vaccination elicited elevated levels of B cell cfDNA, likely reflecting affinity maturation, which correlated with neutralizing antibodies and memory B cells. cfDNA biomarkers provide unique information on immune cell turnover in response to vaccination.

Translation to Patients

Ilana Fox-Fisher, Sheina Piyanzin, Mayan Briller, ..., Ruth Shemer, Dana Wolf, Yuval Dor

yuvald@ekmd.huji.ac.il

Highlights

cfDNA-based monitoring of immune cell turnover following SARS-CoV-2 vaccination

B cell cfDNA levels correlate with neutralizing antibodies and memory B cell counts

Lymphocyte and monocyte cfDNA levels are dramatically elevated after the booster

Fox-Fisher et al., Med 3, 468–480
July 8, 2022
https://doi.org/10.1016/j.medj.2022.05.005

CellPress

Med

Clinical and Translational Article

B cell-derived cfDNA after primary BNT162b2 mRNA vaccination anticipates memory B cells and SARS-CoV-2 neutralizing antibodies

Ilana Fox-Fisher,[1] Sheina Piyanzin,[1] Mayan Briller,[2] Esther Oiknine-Djian,[3] Or Alfi,[3] Roni Ben-Ami,[1] Ayelet Peretz,[1] Daniel Neiman,[1] Bracha-Lea Ochana,[1] Ori Fridlich,[1] Zeina Drawshy,[1] Agnes Klochendler,[1] Judith Magenheim,[1] Danielle Share,[1] Ran Avrahami,[1] Yaarit Ribak,[4] Aviv Talmon,[4] Limor Rubin,[4] Neta Milman,[2] Meital Segev,[2] Erik Feldman,[2] Yuval Tal,[4] Shai S. Shen-Orr,[2] Benjamin Glaser,[5] Ruth Shemer,[1] Dana Wolf,[3] and Yuval Dor[1,*]

ABSTRACT

Background: Much remains unknown regarding the response of the immune system to severe acute respiratory syndrome coronavirus-2 (SARS-CoV-2) vaccination.

Methods: We employed circulating cell-free DNA (cfDNA) to assess the turnover of specific immune cell types following administration of the Pfizer/BioNTech vaccine.

Findings: The levels of B cell cfDNA after the primary dose correlated with development of neutralizing antibodies and memory B cells after the booster, revealing a link between early B cell turnover—potentially reflecting affinity maturation—and later development of effective humoral response. We also observed co-elevation of B cell, T cell, and monocyte cfDNA after the booster, underscoring the involvement of innate immune cell turnover in the development of humoral and cellular adaptive immunity. Actual cell counts remained largely stable following vaccination, other than a previously demonstrated temporary reduction in neutrophil and lymphocyte counts.

Conclusions: Immune cfDNA dynamics reveal the crucial role of the primary SARS-CoV-2 vaccine in shaping responses of the immune system following the booster vaccine.

Funding: This work was supported by a generous gift from Shlomo Kramer. Supported by grants from Human Islet Research Network (HIRN UC4DK116274 and UC4DK104216 to R.S. and Y.D.), Ernest and Bonnie Beutler Research Program of Excellence in Genomic Medicine, The Alex U Soyka Pancreatic Cancer Fund, The Israel Science Foundation, the Waldholtz/Pakula family, the Robert M. and Marilyn Sternberg Family Charitable Foundation, the Helmsley Charitable Trust, Grail, and the DON Foundation (to Y.D.). Y.D. holds the Walter and Greta Stiel Chair and Research Grant in Heart Studies. I.F.-F. received a fellowship from the Glassman Hebrew University Diabetes Center.

INTRODUCTION

mRNA vaccines for severe acute respiratory syndrome coronavirus-2 (SARS-CoV-2) have shown a dramatic success in reducing infections and severe disease. Prime-boost administration of vaccines containing spike mRNA within lipid nanoparticles leads to massive production of anti-spike neutralizing antibodies in most individuals,

Context and significance

To understand the turnover of immune cells following SARS-CoV-2 vaccination, Fox-Fisher et al. analyzed fragments of cell-free DNA (cfDNA) that are released from dying immune cells to blood. The levels of B cell cfDNA after the primary dose correlated with neutralizing antibodies and memory B cells after the booster, revealing that early B cell turnover—potentially reflecting affinity maturation—affects later development of effective antibodies. They also observed co-elevation of lymphocyte and monocyte cfDNA after the booster, underscoring the involvement of innate immune cell turnover in the development of humoral and cellular adaptive immunity. cfDNA biomarkers open a new window into human immune cell dynamics in response to perturbations.

combined with a T cell response.[1] This results in ~90% reduction in the likelihood of infection and 97% reduction in the likelihood to develop severe coronavirus disease 2019 (COVID-19),[2–4] although certain mutations in the spike protein reduce effectiveness of the vaccine.[5] Many open questions remain regarding the processes underlying the response of the immune system to the vaccine, with important practical implications for current vaccine management and the development of future vaccines. For example, considerable inter-individual variation is observed in the quality of the response to the vaccine, with regard to titers of neutralizing antibodies as well as their decline over time.[6–8] At present, the mechanisms governing this heterogeneity are not clear.

Systems immunology analyses using immune cell counts, leukocyte transcriptomes, and antibody measurement have begun to describe the immune processes and circuits taking place following vaccination. Key findings so far are the enhancement of an innate immune response after the booster, seen as elevated monocyte counts and an increased anti-viral interferon response;[9] the induction of a persistent germinal center B cell response;[10] and the observation that elderly individuals elicit a weaker response to the vaccine, including lower levels of neutralizing antibodies and lower levels of spike-specific memory B cells.[8] While these studies provide critical snapshots of the immune response to the vaccine, they have not addressed mechanistic aspects of heterogeneity, and have not identified early individual responses that predict the outcome of vaccination.

Dying cells release short-lived fragments of genomic DNA to the circulation. Circulating cell-free DNA (cfDNA), the substrate of liquid biopsies, has been used extensively to detect fetal chromosomal aberrations,[11–13] to monitor tumor dynamics,[14] and to identify rejection of transplanted organs.[15,16] More recently, tissue-specific epigenetic marks have allowed use of liquid biopsies for the monitoring of tissue turnover in genetically normal cell types.[17–22] We and others have taken advantage of DNA methylation patterns, which are stable and universal characteristics of distinct cell types, and are retained on cfDNA. Tissue-specific DNA methylation patterns can inform on tissue turnover indicative of tumor development,[17,23] on massive cell death (e.g., elevated cardiomyocyte cfDNA after myocardial infarction),[24] and on immune and inflammatory processes involving cell turnover.[25,26] An important feature of cfDNA is its short half-life, estimated at 15–120 min.[27] This means that cfDNA molecules represent cell death events that took place shortly before sampling, and can open an early window into processes that manifest much later as reduced cell counts or tissue mass.

To gain insight into the dynamics of the immune system following prime-boost SARS-CoV-2 vaccination, we collected longitudinal blood counts and serology samples from 100 volunteers who received two doses of the Pfizer/BioNTech mRNA vaccine BNT162b, and characterized changes in immune-derived plasma cfDNA. Here we describe the observed changes and their correlation to established measures of the immune response to the vaccine.

RESULTS

Longitudinal monitoring of blood cells, immune cfDNA, and antibodies following BNT162b2 vaccination

We recruited 100 healthy volunteers (aged 19–78 years, median 40 years) who had received the BNT162b2 vaccine in late December 2020 at the Hadassah Medical Center. Blood samples were drawn from each volunteer just prior to the primary vaccine, and on days 3, 7, 14, 21 (just prior to the booster vaccine), 24, 28, and 42

[1]Department of Developmental Biology and Cancer Research, The Institute for Medical Research Israel-Canada, The Hebrew University-Hadassah Medical School, Jerusalem, Israel

[2]Faculty of Medicine, Technion - Israel Institute of Technology, Haifa, Israel

[3]Clinical Virology Unit, Department of Clinical Microbiology and Infectious Diseases, Hadassah-Hebrew University Medical Center, Jerusalem, Israel

[4]Allergy and Clinical Immunology Unit, Department of Medicine, Jerusalem, Israel

[5]Endocrinology and Metabolism Service, Hadassah Medical Center and Faculty of Medicine, Hebrew University of Jerusalem, Jerusalem, Israel

*Correspondence: yuvald@ekmd.huji.ac.il

https://doi.org/10.1016/j.medj.2022.05.005

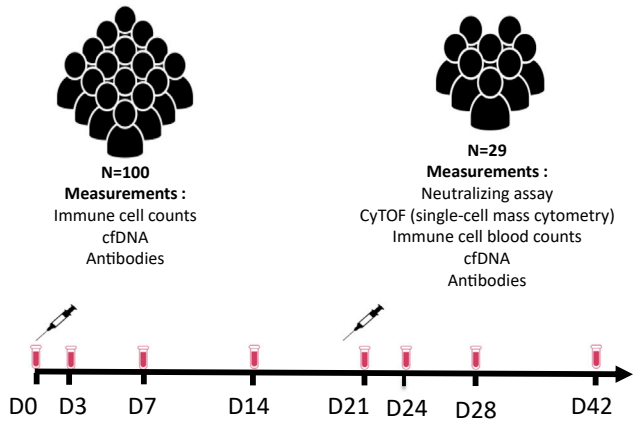

Figure 1. Study design

We recruited 100 volunteers that received the BNT162b2 vaccination (60 females, 40 males, age range 19–78 years, median age 40 years) and obtained blood samples at eight time points before and after vaccination. All samples were assessed for immune cell counts, anti-spike IgG antibodies, and cfDNA markers. A subset of donors (N = 29) were more comprehensively characterized, including neutralizing antibody assay and single-cell mass cytometry (CyTOF). All participants received the booster 3 weeks after the primary vaccine.

(Figures 1 and S1). We obtained complete blood counts (CBCs), measured anti-spike antibodies, extracted DNA from whole blood as well as from plasma, and recorded self-reports on adverse events (Figure S1; Data S1). On a subset of volunteers (n = 29), we also measured SARS-CoV-2 neutralizing antibodies, which are key mediators of protection[6] and used single-cell mass cytometry (cytometry by time of flight [CyTOF]) to assess the levels of dozens of cell surface markers (manuscript in preparation).

We then treated the extracted DNA with bisulfite, amplified it using a cocktail of 12 immune-derived DNA methylation markers (Figure S2; Table S1[26]), and sequenced the products as described[28] to quantify the presence of DNA from specific immune cell types. The cocktail includes genomic loci, each of which is uniquely unmethylated in DNA from a specific immune cell type: neutrophils, monocytes, B cells, T cells, and CD8 T cells. When applied to genomic DNA extracted from whole blood, these markers provide an accurate estimate of white blood cell (WBC) counts;[26,29] indeed, we observed a good correlation between cell counts measured by CBC or CyTOF, and cell counts defined by DNA methylation analysis of genomic DNA from whole blood (Figure S2). Importantly, when applied to cfDNA, these methylation markers reflect immune cell type-specific turnover, which may anticipate changes in total cell number of a given population.[25,26]

Second dose of vaccine elicits a dramatic elevation of cfDNA derived from both adaptive and innate immune cells

Total counts of WBCs, as well as the numbers of B cells, T cells, monocytes, and neutrophils, assessed using either CBCs or methylation markers in genomic DNA from whole blood, remained relatively stable during the 42 days that followed the primary dose. We noticed a small and transient drop in total WBC counts as well as neutrophil, B, and T cell counts on day 24 (3 days after the booster), followed by elevated T cell counts on day 28 (Figures 2A and S3A–S3C). Transient neutropenia has been reported previously following administration of other vaccines,[30] and BNT162b2 has been reported to cause a transient reduction in lymphocyte counts, attributed to interferon-induced redistribution of lymphocytes into lymphoid tissues.[31]

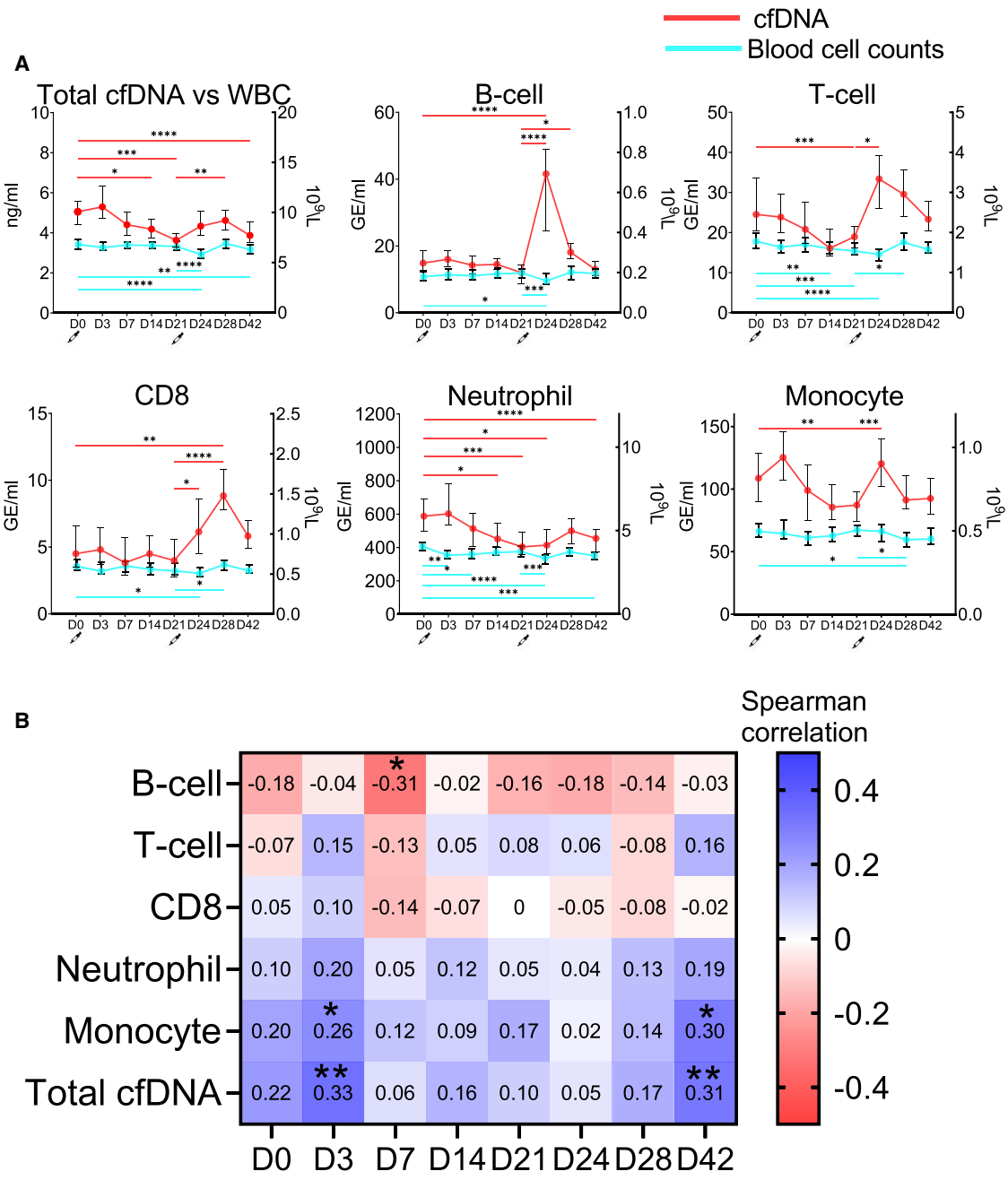

Figure 2. Temporal changes in innate and adaptive immune cfDNA and cell counts following vaccination

(A) Total cfDNA (ng/mL), immune-derived cfDNA (GE/mL) (red lines), and circulating immune cells (10^9/ L) (light blue lines) following vaccination. Immune cell counts were calculated using methylation marker analysis on genomic DNA extracted from whole blood. Statistical differences were tested between each time point and baseline (D0), and between days 24–42 and day 21 (just prior to the second vaccination). p values calculated using mixed-effects analysis. *p < 0.05, **p > 0.01, ***p < 0.001, ****p < 0.0001. Bars, median; error bars, 95% confidence interval (CI).

(B) A heatmap of the Spearman rank correlation of immune-derived cfDNA from each cell type and age (red, negative correlation; blue, positive correlation). Numbers within boxes are correlation coefficients.

Interestingly, we observed that T cell-, B cell-, neutrophil-, and monocyte-derived cfDNA concentrations (as well as total cfDNA levels) decreased transiently on days 14 and 21 following the priming dose (Figure 2A). The change was more evident when each sample was normalized to cfDNA levels of the same donor

prior to vaccination (Figure S3D). These findings may result from more rapid clearance of cfDNA, or alternatively from a hitherto-unrecognized process of attenuated immune cell turnover in response to the priming vaccine dose. We favor the latter explanation as it is consistent with, and can be the reason for, the observed reduction in cell counts on day 24. Additional experiments will be required to determine the basis for the transient decrease in cfDNA levels following vaccination.

Strikingly, the concentrations of cfDNA derived from B cells, T cells, CD8 T cells, and monocytes were co-elevated on after the booster ($p < 0.0001$, mixed-effects analysis), revealing a rapid, coordinated response of the adaptive and innate immune systems to the second dose (Figures 2A, S3D, and S3E). B cell cfDNA was most significantly increased (median change, 2.7-fold) followed by T cell cfDNA (median change, 1.7-fold) and monocyte cfDNA (median change, 1.47-fold), and all peaked on day 24 (3 days after the booster) and declined thereafter. Interestingly, $CD8^+$ T cell cfDNA peaked later, on day 28 (Figures 2A and S4A). The elevation of cfDNA levels after the booster was accompanied by a transient reduction in B cell, neutrophil, and total leukocyte counts.

We asked if changes of cfDNA levels derived from each cell type occur independently (for example, B cell cfDNA levels fluctuating independently of the levels of neutrophil cfDNA), or in a coordinated manner. A correlation matrix revealed that immune-derived cfDNA levels were in fact highly correlated throughout the study period. That is, when B cell cfDNA levels increased in an individual, the levels of cfDNA from T cells, monocytes, and neutrophils were also likely to increase (Figure S4B). This suggests that vaccination results in a simultaneous, coordinated turnover response of the innate and adaptive immune systems.

Last, we assessed cfDNA responses as a function of the age of vaccinees. Strikingly, B cell cfDNA levels on day 7 were negatively correlated with age, while the levels of monocyte cfDNA and total cfDNA on days 3 and 42 were positively correlated with age (Figure 2B). This finding suggests that the process of aging attenuates the turnover of B cells in response to vaccination, potentially contributing to the weaker antibody response reported previously in the elderly,[8,32] while it causes a stronger response of the innate immune system to the vaccine.

Immune cfDNA levels anticipate antibody production

We next sought to correlate the profiles of cfDNA in response to vaccination to the intended functional consequence, namely antibody production. Consistent with previous reports,[31–33] primary vaccination led to a dramatic elevation in the concentration of anti-spike antibodies, which was further elevated after the booster, and started to plateau on day 42 (Figure 3A).

We observed that the levels of B cell-derived cfDNA on days 0 and 3 did not correlate with the levels of antibodies measured at any day ($p > 0.29$). However, B cell cfDNA levels on days 7, 14, and 24 were weakly but significantly correlated ($r = 0.28–0.47$, $p = 0.03–0.05$ Spearman correlation; Benjamini–Hochberg [BH]adjusted p value) to the levels of antibodies measured in the same individual 4–7 days later (on days 14, 21, and 28, respectively) (Figure 3B). cfDNA from other immune cell types did not correlate significantly with immunoglobulin (Ig) G levels, other than a weak negative correlation between neutrophil cfDNA on days 0 and 3 and antibody levels (Figure S5). Breaking down the cohort of vaccinees by age groups (above and below 40 years, a cutoff consistent with observations made in a previous study),[26] we

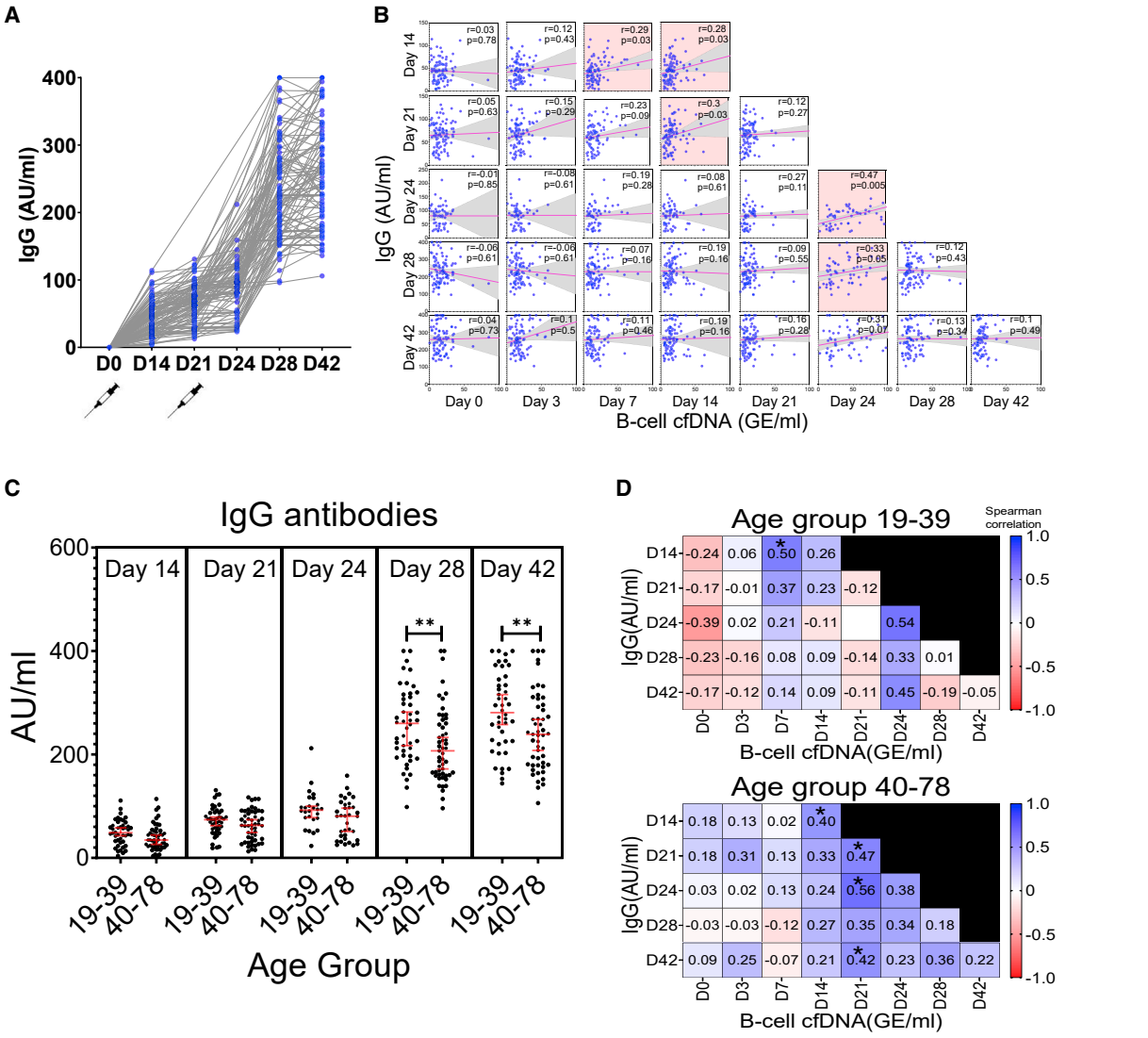

Figure 3. Correlation between B cell cfDNA dynamics and antibody production

(A) Measurements of anti-spike IgG antibody following administration of BNT162b2 (a.u./mL).

(B) Correlation between B cell-derived cfDNA (GE/mL) and anti-spike IgG (a.u./mL). Pink line shows simple linear regression, gray background CI 95%. Spearman correlation; Benjamini-Hochberg-adjusted p value to correct for multiple testing; false discovery rate (FDR) 5%. Red background shows correlations that are statistically significant($p < 0.05$).

(C) Levels of anti-spike IgG antibody as a function of time, divided into age groups (19–39 years, n = 47; 40–78 years, n = 48). Mann-Whitney U test. *$p < 0.05$, **$p > 0.01$, ***$p < 0.001$, ****$p < 0.0001$. Bars, median; error bars, 95% confidence interval (CI).

(D) A heatmap of Spearman's correlation between B cell-derived cfDNA (GE/mL) and anti-spike IgG (a.u./mL) in the two age groups. Benjamini-Hochberg-adjusted p value; FDR 5%. Numbers are correlation coefficients.

observed that individuals above 40 years had, on average, a lower titer of anti-spike IgG antibodies ($p < 0.0018$, Mann-Whitney test) (Figure 3C), as reported.[8,32] We measured how B cell cfDNA correlated with subsequent antibody production in young and old donors. Interestingly, the young but not the older donors showed a significant correlation between B cell cfDNA on day 7 and antibody titer on day 14 (Figure 3D), suggesting a faster functional response to the vaccine in younger individuals. In older (but not in young) individuals, B cell cfDNA levels on day 21 correlated with subsequent antibody production, potentially reflecting a slower process of affinity maturation in the old, even when productive (Figure 3D).

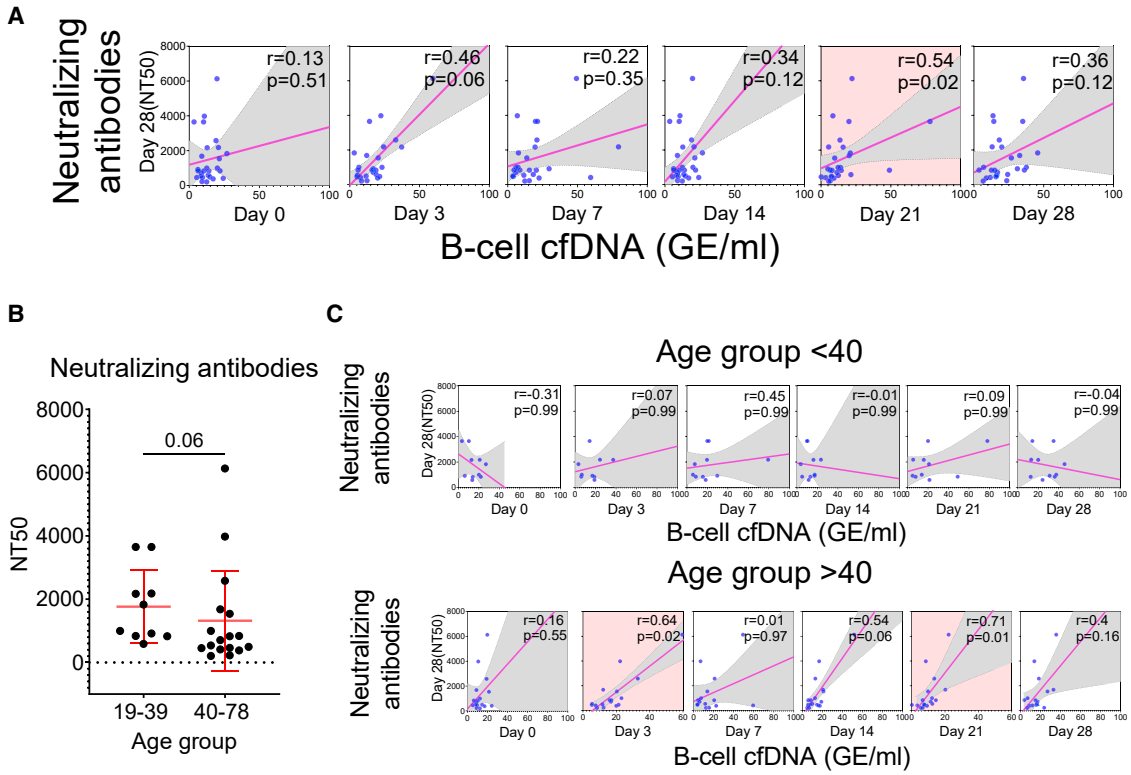

Figure 4. Correlation between B cell cfDNA dynamics and day 28 neutralizing antibodies

(A) Spearman's correlation between B cell-derived cfDNA and neutralizing antibodies on day 28 (NT50).

(B) Day 28 neutralizing antibodies divided by age (p = 0.06, Mann-Whitney U test).

(C) Age dependency of the Spearman's correlation between B cell-derived cfDNA (GE/mL) and day 28 neutralizing antibodies (NT50). Red line shows simple linear regression, gray background CI 95%. Spearman correlation test, p value is corrected for multiple testing BH FDR 5%. Pink marks panels with statistically significant correlations($p < 0.05$).

We further determined the levels of neutralizing antibodies in a subset of 29 volunteers, on day 28 (7 days after the booster). As reported,[31,34] IgG levels on day 14 and beyond were correlated with neutralizing antibodies (Figure S6). The levels of neutralizing antibodies on day 28 were positively correlated with B cell-derived cfDNA levels a week earlier, on day 21 (r = 0.54, p = 0.02, Spearman correlation; BH-adjusted p value), providing further evidence that changes in B cell turnover in a given individual in response to the primary vaccination anticipate antibody production after the booster (Figure 4A). The correlation was specific to B cell turnover, as the levels of cfDNA derived from T cells, monocytes, and neutrophils did not correlate with neutralizing antibodies (Figure S6). Similar to the situation with the titer of anti-spike antibodies, neutralizing antibody activity was lower in individuals older than 40 years (Figure 4B). Interestingly, B cell cfDNA levels on days 3 and 21 anticipated neutralizing antibodies on day 28, in the older group (r = 0.64–0.71, p = 0.01–0.02, Spearman correlation; BH-adjusted p value) but not in the younger group (Figure 4C).

These findings provide the first evidence that measurable B cell turnover dynamics in individuals are predictive of antibody production.

B cell cfDNA anticipates memory B cell production

Stimulation of B cells leads to differentiation of antibody-producing plasma cells, as well as formation of memory B cells that account for long-lasting immune memory. To assess the numbers of plasmablasts and memory B cells, we applied CyTOF to

blood samples from 29 of the vaccinees, using antibodies against CD20, CD27, and CD38 as surrogate markers (see STAR Methods). The total number of memory B cells and plasmablasts did not change following vaccination (Figures S7A and S7B).

To understand the relationship between cfDNA changes and cell formation, we tested the correlation of B cell cfDNA with the measured B cell subsets. We observed that the number of plasmablasts did not correlate with measurements of B cell cfDNA at any day. However, the concentration of B cell-derived cfDNA on day 14 did correlate with the number of memory B cells on days 21 and 28 ($r = 0.59–0.6$, $p = 0.02$, Spearman correlation; BH-adjusted p value), suggesting that increased cell turnover led to increased cell abundance (Figures 5A and 5B).

The concentration of B cell-derived cfDNA on day 14 was significantly correlated with the number of memory B cells at later time points (day 14 to day 28) in vaccinees of both age groups (above and below 40 years), and the correlation resisted a correction for age (Figures 5C and 5D). In contrast, the well-established correlation between memory B cells and the titer of neutralizing antibodies[8,32,35] was eliminated when we corrected for age (Figures S7C–S7F). These findings suggest that the relationship between B cell cfDNA and subsequent memory B cell counts is not explained simply by an age confounder. Thus, the extent of B cell turnover 14 days after the priming dose of vaccine, as reflected in B cell cfDNA, predicts the magnitude of memory B cell formation in the time that follows, regardless of variations in the effect of the booster. Taken together, our findings show that an individual's B cell response to the priming vaccine dose is an important correlate of the formation of both neutralizing antibodies and memory B cells.

DISCUSSION

The mRNA vaccine to SARS-CoV-2 elicits a robust immune response that provides excellent, albeit temporary, protection from COVID-19. To understand the inter-individual variation in the response to the vaccine and predict its outcome, we employed a novel analyte: immune-derived cfDNA. Several features of this analyte endow it with unique information regarding immune system dynamics. First, cfDNA can be assigned to a specific cell type of origin using highly conserved DNA methylation patterns. Second, circulating fragments of genomic DNA are derived from dying cells, and hence provide an insight into cell death dynamics, distinct from the information present in cell counts, which reflect both cell death and cell production. Third, cfDNA fragments reach systemic circulation even when their site of origin is not within the circulation, and therefore can report on processes taking place in remote locations (e.g., cell death within germinal centers). Fourth, cfDNA molecules are cleared from blood within minutes,[14,36] so their concentration reflects contemporary rather than historical cell death events. Last, changes in the rate of cell turnover as reflected by cfDNA can anticipate slower dynamics occurring in cell number. This principle is well established in cancer, where tumor growth can be anticipated from elevated levels of tumor-derived cfDNA,[19,23] and is true also for immune cell dynamics.[26]

Based on these principles, we searched for post-vaccination processes that correlate with, and can be predicted by, immune-derived cfDNA dynamics. The key finding is that elevated B cell-derived cfDNA after the priming vaccine dose correlates with the efficiency of neutralizing antibody activity against SARS-CoV-2, as well as the formation of memory B cells, both measured after the booster. This suggests that an individual's B cell turnover activity in response to the primary

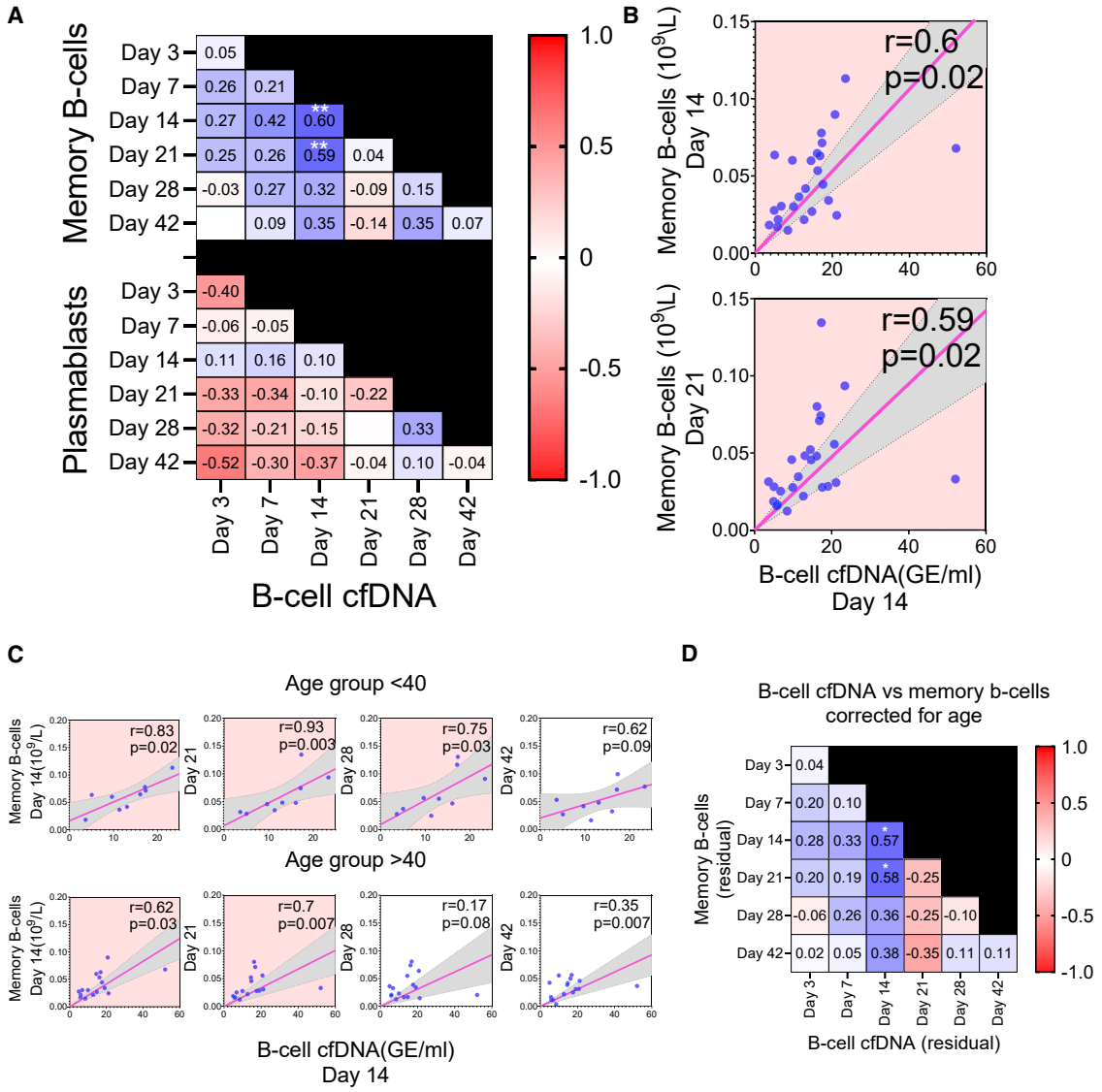

Figure 5. B cell cfDNA an early indicator of memory B cell production

(A) A heatmap of Spearman's correlation between levels of B cell-derived cfDNA and memory B cells (top) or plasmablasts (bottom), as measured by CyTOF (10^9/L).

(B) Detailed view of statistically significant correlations in the heatmap in (A).

(C) Spearman's correlation between day 14 B cell-derived cfDNA (GE/mL) and memory B cells (10^9/L), divided by age groups. Red line, linear regression. Gray background, CI 95%. p value is corrected for multiple testing BH FDR 5%. Pink marks panels with statistically significant correlations($p<0.05$).

(D) A heatmap of Spearman's correlation between B cell cfDNA and memory B cells, corrected for age. Asterisks denote statistical significance. *$p < 0.05$, **$p > 0.01$, ***$p < 0.001$, ****$p < 0.0001$.

vaccine (but not baseline B cell turnover) is crucial in shaping the quality of the humoral response, as manifested after the booster. We hypothesize that the link between elevated B cell cfDNA, production of neutralizing antibodies, and formation of memory B cells is affinity maturation, taking place in germinal centers. In this process, antigen-binding B cells undergo rounds of proliferation, somatic hypermutation, and clonal selection. Cells with improved affinity to the target epitope are selected to become plasma cells or memory B cells, while other cells die off, likely releasing to circulation DNA fragments that carry B cell methylation signatures. The central role of affinity maturation is consistent with the recent

observation that mutation burden in B cells from vaccinees is higher in clones with higher affinity to the S protein, suggesting memory B cell origin rather than plasma cells.[10] Thus, we propose that the levels of B cell cfDNA reflect the intensity of affinity maturation, which is causal in generating neutralizing antibodies and memory B cells. Further studies are needed to examine this concept.

Notably, the correlation between the levels of B cell cfDNA and later production of neutralizing antibodies and memory B cells is partial, suggesting that additional pre-existing or vaccine-elicited parameters participate in shaping immune response to the vaccine. Among these factors, age may play a role, as older individuals had a weaker B cell turnover following vaccination, which correlated with lower titers of neutralizing antibodies.

We acknowledge that the ability to predict vaccination outcome from B cell cfDNA levels should be validated in independent experimental cohorts. Nonetheless, several lines of evidence support validity of the proposed link between B cell cfDNA and vaccination outcome. First, the correlation was specific to cfDNA derived from B cells, the most biologically relevant cell type. Second, B cell cfDNA was correlated with two independently measured parameters of vaccination outcome, namely memory B cells and neutralizing antibodies. Third, we have observed a similar phenomenon among individuals that received an influenza vaccine: people that failed to elevate B cell cfDNA after vaccination were more likely to be non-responders and fail to produce high titers of anti-hemagglutinin antibodies.[26]

Taken together, the findings suggest that the quality of the immune response to the vaccine can, in principle, be predicted by measurements taken shortly after the primary vaccine, potentially adjusting vaccine regime in near real time to ensure a successful response of all vaccinees.

T cells also undergo a process of maturation upon exposure to cells expressing the introduced antigen, resulting in the formation of effector and effector memory T cells.[37] Although these responses are more difficult to measure than the humoral response, the dynamics of T cell-derived cfDNA post vaccination suggest that cfDNA can be informative regarding the development of cellular immunity as well.

Concerning the booster, we found that it elicited a concomitant elevation of cfDNA derived from lymphocytes (T and B cells) and monocytes/macrophages. The most likely interpretation is that the booster triggers massive proliferation of all immune cell types, accompanied and balanced by massive cell death. Consequently, total cell numbers do not change, although intra-population composition (e.g., sub-types of neutrophils) may change. The nature of this process is not clear, but it is consistent with a coordinated innate-adaptive immune response recorded after the booster in the form of elevated interferon gamma in plasma, and an increase in inflammatory monocytes.[9] We note that, even in response to the primary dose, changes in the levels of cfDNA from different immune cell types were highly correlated, further supporting the idea that innate and adaptive immune responses are tightly coordinated.

In summary, using cfDNA methylation markers, we infer immune cell turnover dynamics in response to BNT162b2. We detect a coordinated innate/adaptive immunity response to the booster that involves massive cell turnover, and identify elevated B cell turnover after the primary vaccine—likely a non-invasive reflection of affinity maturation within germinal centers—as an important determinant of varied quality of the eventual immune response.

Limitations of the study

This study has several notable limitations. Most fundamentally, DNA methylation is a characteristic of stable cell types, rather than dynamic cell states. The resolution of methylation markers reflects this inherent biology of DNA methylation, although it can certainly be increased to distinguish between more cell types than our current crude definitions. Notably, other epigenetic marks can potentially report on gene expression programs within cells that released cfDNA.[22] Second, we recognize that one of the major outcome measures used in this study—counting memory B cells—used a proxy definition (cell surface expression of CD20/27/38) rather than a true functional definition, which is not available at this time, and without demonstration of SARS-CoV-2 specificity. Third, the study was not designed to assess cfDNA correlates of protection from infection or disease, forcing us to focus on the available readout of antibodies and memory B cells. Follow-up studies are needed to validate the findings described here and address limitations to achieve a fuller understanding of individual heterogeneity in the response to COVID-19 vaccine.

STAR★METHODS

Detailed methods are provided in the online version of this paper and include the following:

- KEY RESOURCES TABLE
- RESOURCE AVAILABILITY
  - Lead contact
  - Materials availability
  - Data and code availability
- EXPERIMENTAL MODEL AND SUBJECT DETAILS
- METHOD DETAILS
  - Immune cell type methylation markers
  - Sample collection
  - Next generation sequencing
  - Antibody measurements
  - Mass cytometry
  - Batch correction of raw CyTOF data
  - Data post-processing
  - Statistical analysis

SUPPLEMENTAL INFORMATION

Supplemental information can be found online at https://doi.org/10.1016/j.medj.2022.05.005.

ACKNOWLEDGMENTS

We thank Idit Shiff and Abed Nasseredin from the Core Research Facility at The Hebrew University Faculty of Medicine for their support in sequencing analysis, and Noa Makhervax and Dr Lilach Gavish for help in coordinating the effort. This work was supported by a generous gift from Shlomo Kramer. Supported by grants from Human Islet Research Network (HIRN UC4DK116274 and UC4DK104216 to R.S and Y.D.); Ernest and Bonnie Beutler Research Program of Excellence in Genomic Medicine, The Alex U Soyka Pancreatic Cancer Fund, The Israel Science Foundation, the Waldholtz/Pakula family, the Robert M. and Marilyn Sternberg Family Charitable Foundation, the Helmsley Charitable Trust, Grail, and the DON Foundation. Y.D. holds the Walter and Greta Stiel Chair and Research Grant in Heart Studies. I.F.-F. received a fellowship from the Glassman Hebrew University Diabetes Center.

AUTHOR CONTRIBUTIONS

Conceptualization, Y.D. and I.F.-F.; investigation, I.F.-F., S.P., M.B., E.O.-D., O.A., N.M., M.S., E.F., R.A., and O.F.; project administration, R.B.-A., A.P., D.N., B.-L.O., O.F., Z.D., A.K., J.M., D.S., Y.R., A.T., and L.R.; supervision, Y.D., R.S., B.G., D.W., Y.T., and S.S.S.-O.; writing – original draft, Y.D. and I.F.-F.; writing – review & editing, R.S., B.G., A.K., D.W., Y.T., and S.S.S.-O. I.F.-F. and R.A. performed statistical analyses. Y.D., I.F.-F. and R.S. had unrestricted access to all data. Y.D. and I.F.-F. prepared the first draft of the manuscript, which was reviewed and edited by all other authors. All authors agreed to submit the manuscript, read and approved the final draft, and take full responsibility for its content, including the accuracy of the data and statistical analysis.

DECLARATION OF INTERESTS

I.F.-F., B.G., R.S., and Y.D. have filed patents related to DNA methylation markers.

Received: October 14, 2021
Revised: February 17, 2022
Accepted: May 12, 2022
Published: May 19, 2022

REFERENCES

1. Lederer, K., Castaño, D., Gómez Atria, D., Oguin, T.H., Wang, S., Manzoni, T.B., Muramatsu, H., Hogan, M.J., Amanat, F., Cherubin, P., et al. (2020). SARS-CoV-2 mRNA vaccines foster potent antigen-specific germinal center responses associated with neutralizing antibody generation. Immunity *53*, 1281–1295.e5. https://doi.org/10.1016/j.immuni.2020.11.009.

2. Haas, E.J., Angulo, F.J., McLaughlin, J.M., Anis, E., Singer, S.R., Khan, F., Brooks, N., Smaja, M., Mircus, G., Pan, K., et al. (2021). Impact and effectiveness of mRNA BNT162b2 vaccine against SARS-CoV-2 infections and COVID-19 cases, hospitalisations, and deaths following a nationwide vaccination campaign in Israel: an observational study using national surveillance data. Lancet *397*, 1819–1829. https://doi.org/10.1016/s0140-6736(21)00947-8.

3. Amit, S., Regev-Yochay, G., Afek, A., Kreiss, Y., and Leshem, E. (2021). Early rate reductions of SARS-CoV-2 infection and COVID-19 in BNT162b2 vaccine recipients. Lancet *397*, 875–877. https://doi.org/10.1016/s0140-6736(21)00448-7.

4. Thompson, M.G., Burgess, J.L., Naleway, A.L., Tyner, H., Yoon, S.K., Meece, J., Olsho, L.E.W., Caban-Martinez, A.J., Fowlkes, A.L., Lutrick, K., et al. (2021). Prevention and attenuation of covid-19 with the BNT162b2 and mRNA-1273 vaccines. N. Engl. J. Med. *385*, 320–329. https://doi.org/10.1056/NEJMoa2107058.

5. Planas, D., Veyer, D., Baidaliuk, A., Staropoli, I., Guivel-Benhassine, F., Rajah, M.M., Planchais, C., Porrot, F., Robillard, N., Puech, J., et al. (2021). Reduced sensitivity of SARS-CoV-2 variant Delta to antibody neutralization. Nature *596*, 276–280. https://doi.org/10.1038/s41586-021-03777-9.

6. Bergwerk, M., Gonen, T., Lustig, Y., Amit, S., Lipsitch, M., Cohen, C., Mandelboim, M., Levin, E.G., Rubin, C., Indenbaum, V., et al. (2021). Covid-19 breakthrough infections in vaccinated health care workers. N. Engl. J. Med. *385*, 1474–1484. https://doi.org/10.1056/nejmoa2109072.

7. Cho, A., Muecksch, F., Schaefer-Babajew, D., Wang, Z., Finkin, S., Gaebler, C., Ramos, V., Cipolla, M., Agudelo, M., Bednarski, E., et al. (2021). Antibody evolution after SARS-CoV-2 mRNA vaccination. Preprint at bioRxiv. https://doi.org/10.1101/2021.07.29.454333.

8. Collier, D.A., Ferreira, I.A.T.M., Kotagiri, P., Datir, R.P., Lim, E.Y., Touizer, E., Meng, B., Abdullahi, A., Baker, S., Elmer, A., et al. (2021). Age-related immune response heterogeneity to SARS-CoV-2 vaccine BNT162b2. Nature *596*, 417–422. https://doi.org/10.1038/s41586-021-03739-1.

9. Arunachalam, P.S., Scott, M.K.D., Hagan, T., Li, C., Feng, Y., Wimmers, F., Grigoryan, L., Trisal, M., Edara, V.V., Lai, L., et al. (2021). Systems vaccinology of the BNT162b2 mRNA vaccine in humans. Nature *596*, 410–416. https://doi.org/10.1038/s41586-021-03791-x.

10. Turner, J.S., O'Halloran, J.A., Kalaidina, E., Kim, W., Schmitz, A.J., Zhou, J.Q., Lei, T., Thapa, M., Chen, R.E., Case, J.B., et al. (2021). SARS-CoV-2 mRNA vaccines induce persistent human germinal centre responses. Nature *596*, 109–113. https://doi.org/10.1038/s41586-021-03738-2.

11. Bianchi, D.W., Lamar Parker, R., Wentworth, J., Madankumar, R., Saffer, C., Das, A.F., Craig, J.A., Chudova, D.I., Devers, P.L., Jones, K.W., et al. (2014). DNA sequencing versus standard prenatal aneuploidy screening. N. Engl. J. Med. *69*, 319–321. https://doi.org/10.1097/01.ogx.0000451481.18231.1b.

12. Fan, H.C., Gu, W., Wang, J., Blumenfeld, Y.J., El-Sayed, Y.Y., and Quake, S.R. (2012). Non-invasive prenatal measurement of the fetal genome. Nature *487*, 320–324. https://doi.org/10.1038/nature11251.

13. Lo, Y.M.D., Corbetta, N., Chamberlain, P.F., Rai, V., Sargent, I.L., Redman, C.W., and Wainscoat, J.S. (1997). Presence of fetal DNA in maternal plasma and serum. Lancet *350*, 485–487. https://doi.org/10.1016/s0140-6736(97)02174-0.

14. Wan, J.C.M., Massie, C., Garcia-Corbacho, J., Mouliere, F., Brenton, J.D., Caldas, C., Pacey, S., Baird, R., and Rosenfeld, N. (2017). Liquid biopsies come of age: towards implementation of circulating tumour DNA. Nat. Rev. Cancer *17*, 223–238. https://doi.org/10.1038/nrc.2017.7.

15. De Vlaminck, I., Valantine, H.A., Snyder, T.M., Strehl, C., Cohen, G., Luikart, H., Neff, N.F., Okamoto, J., Bernstein, D., Weisshaar, D., et al. (2014). Circulating cell-free DNA enables noninvasive diagnosis of heart transplant rejection. Sci. Transl. Med. *6*, 241ra77. https://doi.org/10.1126/scitranslmed.3007803.

16. De Vlaminck, I., Martin, L., Kertesz, M., Patel, K., Kowarsky, M., Strehl, C., Cohen, G., Luikart, H., Neff, N.F., Okamoto, J., et al. (2015). Noninvasive monitoring of infection and rejection after lung transplantation. Proc. Natl. Acad. Sci. U S A *34*, S137–S13341. https://doi.org/10.1016/j.healun.2015.01.368.

17. Lehmann-Werman, R., Neiman, D., Zemmour, H., Moss, J., Magenheim, J., Vaknin-Dembinsky, A., Rubertsson, S., Nellgård, B., Blennow, K., Zetterberg, H., et al. (2016). Identification of tissue-specific cell death using methylation patterns of circulating DNA. Proc. Natl. Acad. Sci. U S A *113*, E1826–E1834. https://doi.org/10.1073/pnas.1519286113.

18. Sun, K., Jiang, P., Chan, K.C.A., Wong, J., Cheng, Y.K.Y., Liang, R.H.S., Chan, W.K., Ma, E.S.K., Chan, S.L., Cheng, S.H., et al. (2015). Plasma DNA tissue mapping by genome-wide

methylation sequencing for noninvasive prenatal, cancer, and transplantation assessments. Proc. Natl. Acad. Sci. U S A *112*, E5503–E5512. https://doi.org/10.1073/pnas.1508736112.

19. Moss, J., Zick, A., Grinshpun, A., Carmon, E., Maoz, M., Ochana, B.L., Abraham, O., Arieli, O., Germansky, L., Meir, K., et al. (2020). Circulating breast-derived DNA allows universal detection and monitoring of localized breast cancer. Ann. Oncol. *31*, 395–403. https://doi.org/10.1016/j.annonc.2019.11.014.

20. Snyder, M.W., Kircher, M., Hill, A.J., Daza, R.M., and Shendure, J. (2016). Cell-free DNA comprises an in vivo nucleosome footprint that informs its tissues-of-origin. Cell *164*, 57–68. https://doi.org/10.1016/j.cell.2015.11.050.

21. Sun, K., Jiang, P., Cheng, S.H., Cheng, T.H.T., Wong, J., Wong, V.W.S., Ng, S.S.M., Ma, B.B.Y., Leung, T.Y., Chan, S.L., et al. (2019). Orientation-aware plasma cell-free DNA fragmentation analysis in open chromatin regions informs tissue of origin. Genome Res. *29*, 418–427. https://doi.org/10.1101/gr.242719.118.

22. Sadeh, R., Sharkia, I., Fialkoff, G., Rahat, A., Gutin, J., Chappleboim, A., Nitzan, M., Fox-Fisher, I., Neiman, D., Meler, G., et al. (2021). ChIP-seq of plasma cell-free nucleosomes identifies gene expression programs of the cells of origin. Nat. Biotechnol. *39*, 586–598. https://doi.org/10.1038/s41587-020-00775-6.

23. Liu, M.C., Oxnard, G.R., Klein, E.A., Swanton, C., Seiden, M.V., Liu, M.C., Oxnard, G.R., Klein, E.A., Smith, D., Richards, D., et al. (2020). Sensitive and specific multi-cancer detection and localization using methylation signatures in cell-free DNA. Ann. Oncol. *31*, 745–759. https://doi.org/10.1016/j.annonc.2020.02.011.

24. Zemmour, H., Planer, D., Magenheim, J., Moss, J., Neiman, D., Gilon, D., Korach, A., Glaser, B., Shemer, R., Landesberg, G., and Dor, Y. (2018). Non-invasive detection of human cardiomyocyte death using methylation patterns of circulating DNA. Nat. Commun. *9*, 1443. https://doi.org/10.1038/s41467-018-03961-y.

25. Moss, J., Magenheim, J., Neiman, D., Zemmour, H., Loyfer, N., Korach, A., Samet, Y., Maoz, M., Druid, H., Arner, P., et al. (2018). Comprehensive human cell-type methylation atlas reveals origins of circulating cell-free DNA in health and disease. Nat. Commun. *9*, 5068. https://doi.org/10.1038/s41467-018-07466-6.

26. Fox-Fisher, I., Piyanzin, S., Ochana, B.L., Klochendler, A., Magenheim, J., Peretz, A., Loyfer, N., Moss, J., Cohen, D., Drori, Y., et al. (2021). Remote immune processes revealed by immune-derived circulating cell-free dna. eLife *10*, e70520.

27. Han, D.S.C., Lo, Y.D., and Lo, Y.M.D. (2021). The nexus of cfDNA and nuclease biology. Trends Genet. *37*, 758–770. https://doi.org/10.1016/j.tig.2021.04.005.

28. Neiman, D., Gillis, D., Piyanzin, S., Cohen, D., Fridlich, O., Moss, J., Zick, A., Oron, T., Sundberg, F., Forsander, G., et al. (2020). Multiplexing DNA methylation markers to detect circulating cell-free DNA derived from human pancreatic β cells. JCI Insight *5*, e136579. https://doi.org/10.1172/jci.insight.136579.

29. Baron, U., Werner, J., Schildknecht, K., Schulze, J.J., Mulu, A., Liebert, U.G., Sack, U., Speckmann, C., Gossen, M., Wong, R.J., et al. (2018). Epigenetic immune cell counting in human blood samples for immunodiagnostics. Sci. Transl. Med. *10*, eaan3508. https://doi.org/10.1126/scitranslmed.aan3508.

30. Muturi-Kioi, V., Lewis, D., Launay, O., Leroux-Roels, G., Anemona, A., Loulergue, P., Bodinham, C.L., Aerssens, A., Groth, N., Saul, A., and Podda, A. (2016). Neutropenia as an adverse event following vaccination: results from randomized clinical trials in healthy adults and systematic review. PLoS One *11*, e0157385. https://doi.org/10.1371/journal.pone.0157385.

31. Sahin, U., Muik, A., Derhovanessian, E., Vogler, I., Kranz, L.M., Vormehr, M., Baum, A., Pascal, K., Quandt, J., Maurus, D., et al. (2020). COVID-19 vaccine BNT162b1 elicits human antibody and TH1 T cell responses. Nature *586*, 594–599. https://doi.org/10.1038/s41586-020-2814-7.

32. Wei, J., Stoesser, N., Matthews, P.C., Ayoubkhani, D., Studley, R., Bell, I., Bell, J.I., Newton, J.N., Farrar, J., Diamond, I., et al.; COVID-19 Infection Survey team (2021). Antibody responses to SARS-CoV-2 vaccines in 45,965 adults from the general population of the United Kingdom. Nature Microbiol. *6*, 1140–1149. https://doi.org/10.1038/s41564-021-00947-3.

33. Lustig, Y., Sapir, E., Regev-Yochay, G., Cohen, C., Fluss, R., Olmer, L., Indenbaum, V., Mandelboim, M., Doolman, R., Amit, S., et al. (2021). BNT162b2 COVID-19 vaccine and correlates of humoral immune responses and dynamics: a prospective, single-centre, longitudinal cohort study in health-care workers. Lancet Respir. Med. *9*, 999–1009. https://doi.org/10.1016/s2213-2600(21)00220-4.

34. Goel, R.R., Apostolidis, S.A., Painter, M.M., Mathew, D., Pattekar, A., Kuthuru, O., Gouma, S., Hicks, P., Meng, W., Rosenfeld, A.M., et al. (2021). Distinct antibody and memory B cell responses in SARSCoV-2 naïve and recovered individuals following mRNA vaccination. Sci. Immunol. *6*, 1–19.

35. Ciocca, M., Zaffina, S., Fernandez Salinas, A., Bocci, C., Palomba, P., Conti, M.G., Terreri, S., Frisullo, G., Giorda, E., Scarsella, M., et al. (2021). Evolution of human memory B cells from childhood to old age. Front. Immunol. *12*, 690534. https://doi.org/10.3389/fimmu.2021.690534.

36. Jiang, P., and Lo, Y.D. (2016). The long and short of circulating cell-free DNA and the ins and outs of molecular Diagnostics. Trends Genet. *32*, 360–371. https://doi.org/10.1016/j.tig.2016.03.009.

37. Oberhardt, V., Luxenburger, H., Kemming, J., Schulien, I., Ciminski, K., Giese, S., Csernalabics, B., Lang-Meli, J., Janowska, I., Staniek, J., et al. (2021). Rapid and stable mobilization of CD8+ T cells by SARS-CoV-2 mRNA vaccine. Nature *597*, 268–273. https://doi.org/10.1038/s41586-021-03841-4.

38. Percivalle, E., Cambiè, G., Cassaniti, I., Nepita, E.V., Maserati, R., Ferrari, A., Di Martino, R., Isernia, P., Mojoli, F., Bruno, R., et al. (2020). Prevalence of SARS-CoV-2 specific neutralising antibodies in blood donors from the lodi red zone in lombardy, Italy, as at 06 april 2020. Euro. Surveill. *25*, 2001031.

39. Alfi, O., Yakirevitch, A., Wald, O., Wandel, O., Izhar, U., Oiknine-Djian, E., Nevo, Y., Elgavish, S., Dagan, E., Madgar, O., et al. (2021). Human nasal and lung tissues infected ex vivo with SARS-CoV-2 provide insights into differential tissue-specific and virus-specific innate immune responses in the upper and lower respiratory tract. J. Virol. *95*, e0013021. https://doi.org/10.1128/jvi.00130-21.

STAR★METHODS

KEY RESOURCES TABLE

REAGENT or RESOURCE	SOURCE	IDENTIFIER
Antibodies		
Metal-111Cd CD4 clone-RPA-T4	Biolegend	Cat# 300541; RRID:AB_2562809
Metal-112Cd CD3 clone-UCHT1	Biolegend	Cat# 300443; RRID:AB_2562808
Metal-114Cd CD45 clone-HI30	Biolegend	Cat# 304045; RRID:AB_2562821
Metal-115In HLADR clone-L243	Biolegend	Cat# 307651; RRID:AB_2562826
Metal-116Cd CD66b clone-6/40c	Biolegend	Cat# 392902; RRID:AB_2728422
Metal-148Nd CD20 clone-2H7	Biolegend	Cat# 302343; RRID:AB_2562816
Metal-150Nd IgD clone-IA6-2	Biolegend	Cat# 348235; RRID:AB_2563775
Metal-151Eu CD123 clone-6H6	Fluidigm	Cat# 3151001; RRID:AB_2661794
Metal-159Tb CD33 clone-WM53	Biolegend	Cat# 303419; RRID:AB_2562818
Metal-162Dy CD27 clone-O323	Biolegend	Cat# 302839; RRID:AB_2562817
Metal-167Er CD38 clone-HIT2	Fluidigm	Cat# 3167001B; RRID:AB_2802110
Metal-173Yb CD19 clone-HIB19	Biolegend	Cat# 302247; RRID:AB_2562815
Metal-174Yb CD8 clone-SK1	Biolegend	Cat# 344727; RRID:AB_2563762
Bacterial and virus strains		
SARS-CoV-2 isolate	BEI resources	NR-52281
Biological samples		
Human plasma samples obtained from vaccinated healthy subjects	This paper	N/A
Human Serum samples obtained from vaccinated healthy subjects	This paper	N/A
Human Whole blood samples obtained from vaccinated healthy subjects	This paper	N/A
Critical commercial assays		
EZ DNA Methylation-Gold	Zymo-research	CAT# D5006
QIAsymphony DNA Midi Kit (96)	QIAGEN	931255
Qubit dsDNA HS Assay Kit	Invitrogen	Q32854
NextSeq 500/550 v2 Reagent Kit	Illumina	20024904
Liaison SARS-CoV-2 S1/S2 IgG	DiaSorin	311450
Architect SARS-CoV-2 IgG II Quant assay	Abbott	N/A
Cell-ID™ 20-Plex Pd Barcoding Kit	Fluidigm	SKU 201060
Experimental models: Cell lines		
VERO E6 cell	ATCC	CRL-1586
Oligonucleotides		
Primers for neutrophils, see Table S1	This paper	N/A
Primers for monocytes, see Table S1	This paper	N/A
Primers for T-cells, see Table S1	This paper	N/A
Primers for CD8, see Table S1	This paper	N/A
Primers for B-cells, see Table S1	This paper	N/A
Deposited data		
Data S1. Data of characteristics, immune derived cfDNA, cell counts and antibodies.	This paper	Mendeley data: https://doi.org/10.17632/5bmb564d8t.1
Software and algorithms		
GraphPad Prism 9.2.0.	GraphPad	N/A
Batch correction - ComBat() function from the sva package [Version 3.40.0].	R [Version 4.2.1]	N/A
normalize.quantiles.use.target() function from the preprocessCore package [Version 1.54.0]. 5)	R [Version 4.2.1]	N/A
the clean_flow_rate() function from the flowCut package [Version 1.3.1], with an alpha set to 0.01; 4)	R [Version 4.2.1]	N/A
cytofCore.concatenateFiles() function from the cytofCore package [Version 0.4].	R [Version 4.2.1]	N/A

RESOURCE AVAILABILITY

Lead contact

Further information and requests for resources and reagents should be directed to and will be fulfilled by the lead contact, Yuval Dor (yuvald@ekmd.huji.ac.il).

Materials availability

Marker coordinates and primer sequences used in this study are listed in the Key resources table.

Data and code availability

- All data reported in this paper is included in the Data S1 and will be shared by the lead contact upon request. Additional Supplemental Items are available from Mendeley Data at: https://doi.org/10.17632/5bmb564d8t.1.
- This paper does not report original code.
- Any additional information required to reanalyze the data reported in this paper is available from the lead contact upon request.

EXPERIMENTAL MODEL AND SUBJECT DETAILS

The characteristics (age, gender and adverse events) of the participants in this study are summarized in the Data S1 and Figure S1. Age, gender, and adverse events was self-reported by the participants. We recruited 100 healthy volunteers who were about to receive a first BNT162b2 vaccine, to participate in the study. Exclusion criteria were an acute illness and a past Covid-19 infection. Volunteers were asked to report any adverse effect following vaccination. Volunteers donated 10 mL of blood on days 0, 3, 7, 14, 21 after the primary dose and 3, 7, 14 days after the booster dose. One volunteer was excluded due to abnormally high levels of B-cell derived cfDNA before receiving the vaccination, potentially reflecting a hidden B-cell related pathology. The study was approved by the institutional Review Board of Hadassah Medical Center. Blood samples were obtained from participants who have provided written informed consent. This study was conducted according to protocols approved by the Institutional Review Board in Hadassah Medical Center: HMO-14-0198. A Method to Diagnose Cell Death Based on Methylation Signature of Circulating Cell-Free DNA. With procedures performed in accordance with the Declaration of Helsinki.

METHOD DETAILS

Immune cell type methylation markers

We used a subset 12 markers out of the collection of immune-derived DNA methylation markers described recently.[26] These included three neutrophil markers, two monocyte markers, 3 B-cell markers, two general T cell markers, and two $CD8^+$ T cell markers. Marker coordinates and primer sequences are provided in Table S1. Briefly, immune-cell-specific methylation candidate biomarkers were selected using comparative methylome analysis, based on publicly available datasets,[25] to identify loci having more than five CpG sites within 150 bp, with an average methylation value for a specific cytosine (present on Illumina 450K arrays) of less than 0.3 in the specific immune cell type of interest and greater than 0.8 in over 90% of tissues and other immune cells. From our previously-described atlas of human tissue-specific methylomes,[17] we identified ~50 CpG sites that are unmethylated in specific immune-cell types and methylated in all other major immune cells and tissues. We selected two to three sites as markers for neutrophils, monocytes, B-cells, T-cells and $CD8^+$ T-cells, and used primers that amplify ~100 bp fragments

surrounding marker CpGs using a multiplex two-step PCR amplification method, as described.[26,28]

Sample collection

Blood samples were collected by routine venipuncture in 10 mL EDTA Vacutainer® tubes up to 4 hours before plasma separation and complete blood count analysis. For cfDNA processing tubes were centrifuged at 1,500×g for 10 minutes at 4 °C. The supernatant was transferred to a fresh 15 mL conical tube without disturbing the cellular layer, and centrifuged again for 10 min at 3000×g. The supernatant was collected and stored at −80°C.

cfDNA was extracted from 2 to 4 mL of plasma using the QIAsymphony liquid handling robot (Qiagen). cfDNA concentration was determined using Qubit double-strand molecular probes kit (Invitrogen).

DNA derived from all samples was treated with bisulfite using EZ DNA Methylation-Gold (Zymo Research) and eluted in 24 μL elution buffer. gDNA was extracted directly from whole blood using the QIAsymphony DNA Midi Kit (Qiagen). Note that gDNA content in such preparations is similar to the gDNA content of white blood cells, since the other components of whole blood - erythrocytes and platelets – contain negligible amounts of DNA.

Next generation sequencing

Pooled PCR products were subjected to multiplex next-generation sequencing (NGS) using the NextSeq 500/550 v2 Reagent Kit (Illumina). Sequenced reads were separated by barcode, aligned to the target sequence, and analyzed using custom scripts written and implemented in R. Reads were quality filtered based on Illumina quality scores. Reads were identified as having at least 80% similarity to the target sequences and containing all the expected CpGs. CpGs were considered methylated if "CG" was read and unmethylated if "TG" was read. Proper bisulfite conversion was assessed by analyzing methylation of non-CpG cytosines. We then determined the fraction of molecules in which all CpG sites were unmethylated. The fraction obtained was multiplied by the concentration of cfDNA measured in each sample, to obtain the concentration of tissue-specific cfDNA from each donor.

Antibody measurements

The levels of specific anti- SARS–CoV-2 spike IgG (Liaison SARS-CoV-2 S1/S2 IgG, DiaSorin, Saluggia, Italy) and receptor binding domain (RBD) IgG (Architect SARS-CoV-2 IgG II Quant assay, Abbott Diagnostics, Chicago, USA) were assessed in serum specimens, and expressed as arbitrary units (AU)/mL. Neutralizing antibody titers against SARS-CoV-2 were measured using a wild-type SARS-CoV-2 virus microneutralization assay as previously described,[38] with minor modifications. Briefly, serial two-fold dilutions of heat inactivated serum samples (starting from 1:10; diluted in DMEM in a total volume of 50 μL) were incubated with an equal volume of viral solution, containing 100 tissue culture infectious dose (TCID50) of SARS-CoV-2 isolate USA-WA1/2020 (NR-52281; obtained from BEI resources) for 1 h in a 96-well plate, at 37 °C in humidified atmosphere with 5% CO_2. The serum-virus mixtures (100 μL; eight replicates of each serum dilution) were then added to a 96-well plate containing a semi-confluent VERO E6 cell monolayer (ATCC CRL-1586; maintained as described.[39] Following 3 days of incubation at 37°C in a humidified atmosphere with 5% CO_2, the cells in each well were scored for viral cytopathic effect (CPE). The neutralization (NT)50 titer was defined as the reciprocal of the highest serum dilution that protected 50% of culture wells from CPE. Positive and

negative serum controls, cell control, and a viral back-titration control were included in each assay.

Mass cytometry

Sample processing. Heparin tubes were incubated at room temperature for 1 h after collection, and 2.5 mL of blood was then transferred to 3 mL of PROT1 stabilizer (SmartTube Inc. San Carlos, CA, USA). After incubation at room temperature for 10 min, the samples were transferred to −80°c for shipment and long-term storage. In addition, several heparin tubes were collected from a 47-year-old healthy female as a control. The samples were aliquoted and stored similarly in PROT1 buffer. Samples were subsequently thawed using Thaw Lyse X1000 concentrate using the manufacturer's instructions and three million cells were prepared in 15 mL tubes. To facilitate sample acquisition and minimize batch effects, samples were barcoded using a Cell-ID™ 20-Plex Pd Barcoding Kit (Fluidigm Inc, San Francisco, CA, USA), washed and pooled. Cells were then stained for extracellular markers (see Key resources table), washed, and fixed in 1.6% paraformaldehyde overnight in 4°c. Prior to data acquisition, samples were incubated at RT in 0.3% Saponin (Sigma) in PBS, with Ir-intercalator (Fluidigm, 1:2000), washed once in cell staining buffer and cell acquisition solution. Cells were diluted to 0.5 million per 1 mL with cell acquisition solution and acquired by CyTOF Helios machine (Fluidigm). Each of the 13 batches contained 19–20 samples, including one control sample. Internal metal isotope bead standards were added for sample normalization to account for decline in mean marker intensity over time, and normalized using CyTOF-build in function.

Batch correction of raw CyTOF data

During our analysis, we discovered a decline in signal intensity over time in four channels. To account for this decline, we performed the following steps, per batch: 1) removed files with significant differences in intensities to the other files within the same batch; 2) removed files with less than 0.5 million cells; 3) Performed a QC analysis using the *clean_flow_rate()* function from the *flowCut* package [Version 1.3.1], with an *alpha* set to 0.01; 4) Quantile normalization was performed for the four aberrant channels (141Pr – CD57, 157Gd – CD45RA, 165Ho – CD28, 174Yb – CD8) in the following manner: for each file in each batch, the first 20 min of the acquisition were determined to be stable and were used as a reference for quantile normalization. Quantile normalization was performed for every 5 min separately using the *normalize.quantiles.use.target()* function from the *preprocessCore* package [Version 1.54.0]. 5) The normalized files were concatenated using the *cytofCore.concatenateFiles()* function from the *cytofCore* package [Version 0.4].

Data post-processing

Data were uploaded to a Cytobank web server for processing and gating of dead cells and normalization beads. Each batch was gated on separately and manually. Cell frequencies were calculated as a percentage of the parent population and Absolute immune cell number was calculated using % of the specific immune cell subset population out of $CD45^+$ cells multiplied by the white blood cell count measured in the CBC.

Data was imported into R for further analysis. When a duplicate sample ran at two different batches, the sample from the first batch was used. Batch correction was performed using the *ComBat()* function from the *sva* package [Version 3.40.0].

All pre- and post-processing steps were performed in R [Version 4.2.1] and RStudio [Version 1.4.1717].

Statistical analysis

To assess correlation between groups we used Spearman's ranked correlation test. To validate the correlation between CyTOF, CBC and methylation markers we used Pearson's correlation. Adjustment for age was done using a simple linear regression model, with age as the independent variable and neutralizing antibodies, memory B-cells and B-cell derived cfDNA as the dependent variable. Residuals were correlated after regression. For multiple testing we corrected p value with Benjamini Hochberg (FDR 5%). To determine significance of differences between groups we used a non-parametric two-tailed Mann-Whitney test. For multiple comparisons, a mixed-effects analysis of repeated measures data was used. P-value was considered significant when <0.05. Statistical analyses performed with GraphPad Prism 9.2.0.